Decision versus compromise for animal groups in motion

Naomi E. Leonard[a,1], Tian Shen[a], Benjamin Nabet[a], Luca Scardovi[b], Iain D. Couzin[c], and Simon A. Levin[c,1]

Departments of [a]Mechanical and Aerospace Engineering and [c]Ecology and Evolutionary Biology, Princeton University, Princeton, NJ 08544; and [b]Department of Electrical and Computer Engineering, University of Toronto, Toronto, ON, Canada M5S 3G4

Contributed by Simon A. Levin, November 8, 2011 (sent for review June 20, 2011)

Previously, we showed using a computational agent-based model that a group of animals moving together can make a collective decision on direction of motion, even if there is a conflict between the directional preferences of two small subgroups of "informed" individuals and the remaining "uninformed" individuals have no directional preference. The model requires no explicit signaling or identification of informed individuals; individuals merely adjust their steering in response to socially acquired information on relative motion of neighbors. In this paper, we show how the dynamics of this system can be modeled analytically, and we derive a testable result that adding uninformed individuals improves stability of collective decision making. We first present a continuous-time dynamic model and prove a necessary and sufficient condition for stable convergence to a collective decision in this model. The stability of the decision, which corresponds to most of the group moving in one of two alternative preferred directions, depends explicitly on the magnitude of the difference in preferred directions; for a difference above a threshold the decision is stable and below that same threshold the decision is unstable. Given qualitative agreement with the results of the previous simulation study, we proceed to explore analytically the subtle but important role of the uninformed individuals in the continuous-time model. Significantly, we show that the likelihood of a collective decision increases with increasing numbers of uninformed individuals.

collective behavior | Kuramoto | coordinated movement

Explaining the ability of animals that move together in a group to make collective decisions requires an understanding of the mechanisms of information transfer in spatially evolving distributions of individuals with limited sensing capability (1–6). In groups such as fish schools and large insect swarms, it is likely that individuals can sense only the relative motion of near neighbors and may not have the capacity to distinguish a well-informed neighbor from the less well informed (2, 3). Further, it is increasingly becoming recognized that the emergent intelligence of a collective may be more reliable than the intelligence provided by a few leaders or well-informed individuals (7–11). This result suggests a subtle but important role in collective decision making for those individuals that have no particular information or preference.

In this paper we define and analyze a continuous-time dynamical system model to examine collective decision making in moving groups of informed and uninformed individuals that are limited to sensing the relative motion of neighbors and adjusting their steering in response. Informed individuals have a preference for one of two alternative directions of motion, whereas uninformed individuals have no preference. The preferences are representative of knowledge of the direction to a food source or of a migration route, etc. The model is motivated by the discrete-time model of ref. 1, which is used to investigate, through computation, mechanisms of decision making and leadership in groups moving in the plane; it extends the continuous-time model of ref. 12, which exhibits only some of the group behaviors observed in the simulations of ref. 1 (compromises but not decisions).

In the discrete-time model of ref. 1 there is no signaling, no identification of the informed individuals, and no evaluation of others' information. Nonetheless, it is shown in ref. 1 that the group can make a collective decision: With two informed subgroups of equal population (one subgroup per preference alternative), a collective decision to move in one of the two preferred directions is made with high probability as long as the magnitude of the preference conflict, i.e., the difference in preferred directions, is sufficiently large. For small conflict, the group follows the average of the two preferred directions. Further, simulations in ref. 13 provide evidence that increasing the population size of uninformed individuals lowers the threshold on magnitude of conflict, making it "easier" for a collective decision to be made.

Simulations of the kind reported in ref. 1 are highly suggestive, but because they contain many degrees of freedom, it is difficult to identify the influences of particular mechanisms. In this paper we present an approximation to the individual-based model (1) that allows deeper analysis into the microscopic reasons for the observed macroscopic behaviors and a broader exploration of parameter space. The model we propose and study is represented by a system of ordinary differential equations. As in the formulation of ref. 12, each agent is modeled as a particle moving in the plane at constant speed with steering rate dependent on interparticle measurements and, for informed individuals, deviation from a preferred direction. In ref. 12 two timescales, observed in the simulations of ref. 1, are formally proved to exist for the system of equations; in the fast timescale, alignment is established within each subgroup of agents with the same preference (or lack of preference), whereas in the slow timescale, the reduced-order model describes the average motion of each of the two informed subgroups and the uninformed subgroup.

In ref. 12 assumptions are made that simplify the analysis. First, examination is restricted to the directional dynamics of the particles. Second, each individual is assumed capable of sensing the relative direction of motion of every other individual in the group; i.e., the social information is globally available. Third, the uninformed subgroup is ignored in the analysis of the slow timescale dynamics. A comprehensive bifurcation analysis is presented of stable and unstable solutions of the reduced-order dynamics; the results provide insights on stable solutions not explored in the simulation study, unstable solutions not easily understood through simulation, and sensitivity to parameters. However, the simplifying assumptions yield a model that produces some but not all of the behavior observed in ref. 1; notably, the group does not select to move as a whole in one of the preferred directions unless a "forgetting feedback" is introduced such that informed individuals gradually lose their preference if they find themselves moving in a direction far from their preference.

The deviation of the results of ref. 12 from those of ref. 1 focuses attention on a small number of assumptions that may be responsible. It is the second and third assumptions of global sensing and neglect of the uninformed individuals that we relax in this paper. We limit sensing and define dynamics that represent the

Author contributions: N.E.L. designed research; N.E.L., T.S., B.N., and L.S. performed research; N.E.L., B.N., and L.S. contributed new reagents/analytic tools; N.E.L., T.S., B.N., L.S., I.D.C., and S.A.L. analyzed data; and N.E.L. and T.S. wrote the paper.

The authors declare no conflict of interest.

[1]To whom correspondence may be addressed. E-mail: naomi@princeton.edu or slevin@princeton.edu.

This article contains supporting information online at www.pnas.org/lookup/suppl/doi:10.1073/pnas.1118318108/-/DCSupplemental.

ECOLOGY

changing sensing neighborhood for each individual. We include the uninformed individuals in our analysis.

With this unique continuous-time model, we show the stability of collective decision making without a forgetting factor, and we derive the critical value of magnitude of conflict that serves as a threshold for a collective decision. Here a collective decision refers to all individuals in one informed subgroup and all uninformed individuals moving together in the informed subgroup's preferred direction; this differs slightly from the definition of a collective decision in ref. 1, where all individuals achieve consensus and decide on a preferred direction.

Our results agree qualitatively with the results of the study based on the more complex discrete-time model of ref. 1; accordingly, we use the continuous-time model to explore the subtle but important role of the uninformed individuals in collective decision making. In particular, we derive the sensitivity of the collective decision making to the population size of the uninformed individuals, showing that increasing numbers of uninformed individuals increases the likelihood that the group will make a collective decision.

Model

The discrete-time model of ref. 1, like the model of ref. 14, considers a group of individuals, each represented as a self-propelled particle in the plane that adjusts its direction of motion in response to the relative motion of local neighbors and random influences. In ref. 14, individuals steer to align with the average direction of others within a circular neighborhood. In ref. 1, individuals also use circular neighborhoods but make it a priority to steer away from any others that are too close. If there are no such very close neighbors, they steer to align and to attract to neighbors that are not quite so close. Informed individuals sum the steering term that derives from measurements of neighbors with a steering term that heads them toward one of two alternative fixed preferred directions. As the individuals move about, relative positions among them can change and thus the local neighborhood of any given individual can change with time.

We model the discrete-time dynamics of ref. 1 with a continuous-time model that looks much like a spatial extension of coupled oscillator dynamics (15, 16). That is, an individual's heading angle, which determines its direction of motion, resembles a phase angle, and the steering laws, which depend on relative headings (and possibly relative positions) of individuals, serve to dynamically couple the phases among the individuals; see refs. 17 and 18. As in ref. 12, we include the alignment steering term but neglect the repulsion and attraction steering terms of ref. 1; we also include a term that couples the heading angle of each informed individual with one of the two fixed preferred directions. The model is similar to that used in ref. 19 to represent a group of coupled spins in a random magnetic field, where each individual oscillator has a randomly assigned "pinning" angle.

Unlike what is done in any of these continuous-time models, we propose a dynamic model for coupling weights. There is some similarity with coupling weights in the linear consensus dynamic model of ref. 20, which change as a static function of relative distance, decaying exponentially with distance. The coupling weights in our model change as a sigmoidal function of the integrated relative distance between neighbors; this dynamic endows individuals with a fading memory of neighbors. The weight dynamics are similar to Hebbian plasticity in neural circuits with a saturation; the latter is a reinforcing process that strengthens effective synapses and weakens ineffective synapses (21).

Additionally, we use relative direction of motion rather than relative spatial distance as a means of determining neighbors. This is justified by our focus on the decision-making dynamics of groups of informed and uninformed individuals that are initially closely aggregated; for an initially aggregated group of individuals, those that head in the same direction remain close whereas those that head in very different directions quickly separate. With our model of neighbors, the steering laws do not depend on spatial position, and we can analyze the dynamics of the heading directions independently. The lower dimensionality of the heading plus coupling weight dynamics compared with the dimensionality of the full spatial dynamics contributes to making the analysis tractable.

Our model is deliberately made deterministic so that we can investigate mechanisms of collective decision making outside of stochasticity. The model studied in ref. 12 is also deterministic, and the stability and bifurcation results of ref. 12 were shown to persist in the presence of randomness in the investigation of ref. 22. Simulations of the model presented here with some randomness suggest similarly that our results are robust (*SI Text*).

Let N be the total number of individuals in a population; each individual is modeled as a particle moving in the plane at constant speed v_c. We denote by angle $\theta_j(t)$ the direction of motion of individual j at time t. Then, the planar velocity of j at time t is $\mathbf{v}_j = (v_c\cos\theta_j(t), v_c\sin\theta_j(t))$.

We associate every individual with one of three subgroups: The N_1 individuals in subgroup 1 have a preference to move in the direction defined by the angle $\bar{\theta}_1$, the N_2 individuals in subgroup 2 have a preference to move in the direction defined by the angle $\bar{\theta}_2$, and the N_3 individuals in subgroup 3 have no preference. We have that $N_1 + N_2 + N_3 = N$.

We define the rate-of-change of direction of motion for each individual in subgroup 1 as

$$\frac{d\theta_j}{dt} = \sin\big(\bar{\theta}_1 - \theta_j(t)\big) + \frac{K_1}{N}\sum_{l=1}^{N} a_{jl}(t)\sin\big(\theta_l(t) - \theta_j(t)\big), \qquad [1]$$

in subgroup 2 as

$$\frac{d\theta_j}{dt} = \sin\big(\bar{\theta}_2 - \theta_j(t)\big) + \frac{K_1}{N}\sum_{l=1}^{N} a_{jl}(t)\sin\big(\theta_l(t) - \theta_j(t)\big), \qquad [2]$$

and in subgroup 3 as

$$\frac{d\theta_j}{dt} = \frac{K_1}{N}\sum_{l=1}^{N} a_{jl}(t)\sin\big(\theta_l(t) - \theta_j(t)\big). \qquad [3]$$

The constant parameter $K_1 > 0$ weights the attention paid to other individuals versus the attention paid to the preferred direction. The dynamic variable $0 \le a_{jl}(t) \le 1$ defines the weight individual j puts on the information it gets from individual l at time t. A value $a_{jl} = 0$ implies that j cannot sense l.

We model the social interaction (coupling) weights $a_{jl}(t)$ as evolving in time according to saturated integrator dynamics that depend on how "close" individuals are from one another, where closeness is defined in terms of relative heading:

$$\begin{aligned} \frac{d\eta_{jl}}{dt} &= K_2\Big(\rho_{jl}(t) - r\Big), \\ a_{jl}(t) &= \frac{1}{1 + e^{-\eta_{jl}(t)}}. \end{aligned} \qquad [4]$$

In the model of Eq. **4**, $\eta_{jl} = \eta_{lj}$ is an integrated variable, the constant parameter $K_2 > 0$ quantifies the speed at which the interaction gains evolve, $\rho_{jl} = |\cos(\frac{1}{2}(\theta_j - \theta_l))|$ gives a measure of synchrony of direction of motion of l and j, and $0 \le r \le 1$ is a chosen fixed threshold representing an individual's sensing range. It holds that $\rho_{jl} = 1$ if l and j move in the same direction and $\rho_{jl} = 0$ if they move in opposite directions. If $\rho_{jl} > r$, then j and l are close enough to sense each other so η_{jl} increases and a_{jl} eventually converges to the maximum interaction strength of 1. If $\rho_{jl} < r$, then j and l are not close enough to sense each other so η_{jl} decreases and a_{jl} eventually converges to 0. Eq. **4** is equivalent to

$$\frac{da_{jl}}{dt} = K_2\left(1 - a_{jl}(t)\right)a_{jl}(t)\left(\rho_{jl}(t) - r\right). \quad [5]$$

Equilibrium solutions correspond to $a_{jl}(t) = 0$ and $a_{jl}(t) = 1$. The state space for the model of Eqs. **1–3** and **5** is compact because each θ_j is an angle and each a_{jl} is a real number in the interval [0, 1].

Results

The model exhibits fast and slow timescale behavior even for moderate values of gains K_1 and K_2. Let $\mathcal{N}_k$ be the subset of indexes corresponding to individuals j in subgroup k for $k = 1, 2, 3$. For an initially aggregated group, the fast dynamics correspond to the individuals in subgroup k (for each $k = 1, 2, 3$), quickly becoming tightly coupled with one another: The coupling weights $a_{jl}(t)$ for $j \in \mathcal{N}_k$ and $l \in \mathcal{N}_k$ converge to 1, and the direction of motion $\theta_j(t)$ for each $j \in \mathcal{N}_k$ converges to a common angle $\Psi_k(t)$. Also, for each pair of subgroups m and n where $m \neq n$ the coupling weights $a_{jl}(t)$ for $j \in \mathcal{N}_m$ and $l \in \mathcal{N}_n$ quickly approach a common value of either 0 or 1. Thus, after the fast transient, individuals in each subgroup move together in the same direction and the coupling between subgroups becomes constant; the slow dynamics describe the evolution of the average direction of each of the three possibly interacting subgroups.

We can formally derive the fast and slow timescale dynamics in the case that $\varepsilon = \max(1/K_1, 1/K_2) << 1$, using singular perturbation theory (23). We define for $k = 1, 2, 3$

$$\Psi_k = \arg\left(\frac{1}{v_c N_k}\sum_{l\in\mathcal{N}_k}\mathbf{v}_l\right),\ \rho_k = \left|\frac{1}{v_c N_k}\sum_{l\in\mathcal{N}_k}\mathbf{v}_l\right|.$$

Then Ψ_k is the average direction of motion of subgroup k and ρ_k is the magnitude of the normalized average speed of subgroup k. The variable ρ_k provides a measure of synchrony of all of the heading directions in subgroup k; if $\rho_k = 1$, then all individuals in subgroup k are heading in the same direction.

For every $j = 1, \ldots, N$ we associate the value of k such that $j \in \mathcal{N}_k$, and we define a variable α_j as a function of $N_k\theta_j - \sum_{l\in\mathcal{N}_k}\theta_l$ so that it quantifies how close the heading of individual j is to the average direction Ψ_k of its subgroup k. Rewriting Eqs. **1–4** in terms of coordinates Ψ_k, α_j, and a_{jl} reveals that the variables Ψ_k evolve at a slow (order 1) rate whereas α_j and a_{jl} evolve at a fast (order $1/\varepsilon$) rate (*SI Text*).

The fast dynamics have a number of isolated solutions. We consider isolated solutions that correspond to $\rho_k = 1$ and $a_{jl} = 1$, for both j and l in subgroup k for $k = 1, 2, 3$. These solutions correspond to those that emerge from groups that are initially aggregated and correspond to every individual j in subgroup k heading in the same direction Ψ_k. It follows that for these solutions, every coupling weight a_{jl} between an individual j in subgroup 1 and an individual l in subgroup 2 takes the same value A_{12}. Likewise, $a_{jl} = A_{13}$ for j in subgroup 1 and l in subgroup 3 and $a_{jl} = A_{23}$ for j in subgroup 2 and l in subgroup 3. Each of A_{12}, A_{13}, and A_{23} can take the value 0 or 1; so there are a total of eight such solutions.

Each of these eight solutions defines an invariant manifold: Each invariant manifold is defined such that if the dynamics start with synchronized subgroups and interconnections between subgroups defined by constants A_{12}, A_{13}, A_{23} each having value of 0 or 1, then they remain so for all time.

We identify the eight manifolds as follows. Manifold $\mathcal{M}_{101}$ is defined by $(A_{12}, A_{13}, A_{23}) = (1, 0, 1)$ and manifold $\mathcal{M}_{110}$ by $(A_{12}, A_{13}, A_{23}) = (1, 1, 0)$. $\mathcal{M}_{101}$ describes the case in which the two informed subgroups 1 and 2 are coupled but the uninformed subgroup 3 is coupled only with informed subgroup 2; $\mathcal{M}_{110}$ describes the symmetric case in which subgroups 1 and 2 are coupled and subgroup 3 is coupled only with subgroup 1. Manifold $\mathcal{M}_{000}$, defined by $(A_{12}, A_{13}, A_{23}) = (0, 0, 0)$, corresponds to decoupled subgroups. Manifold $\mathcal{M}_{010}$ is defined by $(A_{12}, A_{13}, A_{23}) = (0, 1, 0)$ where the coupling is between informed subgroup 1 and the uninformed subgroup 3 as shown in Fig. 1, *Left*. Manifold $\mathcal{M}_{001}$, defined by $(A_{12}, A_{13}, A_{23}) = (0, 0, 1)$, describes the case symmetric to $\mathcal{M}_{010}$, where the coupling is between informed subgroup 2 and the uninformed subgroup 3 as shown in Fig. 1, *Right*. Manifold $\mathcal{M}_{100}$, defined by $(A_{12}, A_{13}, A_{23}) = (1, 0, 0)$, corresponds to coupling only between the two informed subgroups 1 and 2. Manifold $\mathcal{M}_{011}$, defined by $(A_{12}, A_{13}, A_{23}) = (0, 1, 1)$, describes the case in which the uninformed subgroup 3 is coupled with each informed subgroup 1 and 2, but the two informed subgroups are not coupled with each other. Manifold $\mathcal{M}_{111}$, defined by $(A_{12}, A_{13}, A_{23}) = (1, 1, 1)$, corresponds to coupling among all three subgroups.

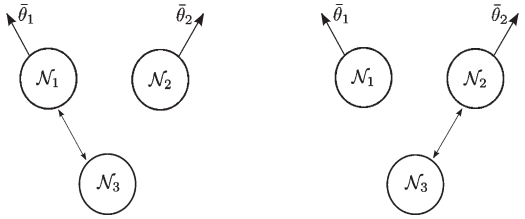

Fig. 1. Coupling in manifolds $\mathcal{M}_{010}$ (*Left*) and $\mathcal{M}_{001}$ (*Right*) among subgroups 1, 2, and 3 as indicated by arrows.

The derived (slow) dynamics on each of the eight manifolds are defined by the rate-of-change of the average direction of motion for each of the three subgroups:

$$\frac{d\Psi_1}{dt} = \sin(\bar{\theta}_1 - \Psi_1(t)) + \frac{K_1}{N}\left(A_{12}N_2\sin(\Psi_2(t) - \Psi_1(t)) + A_{13}N_3\sin(\Psi_3(t) - \Psi_1(t))\right)$$

$$\frac{d\Psi_2}{dt} = \sin\left(\bar{\theta}_2 - \Psi_2(t)\right) + \frac{K_1}{N}\left(A_{12}N_1\sin(\Psi_1(t) - \Psi_2(t)) + A_{23}N_3\sin(\Psi_3(t) - \Psi_2(t))\right)$$

$$\frac{d\Psi_3}{dt} = \frac{K_1}{N}\left(A_{13}N_1\sin(\Psi_1(t) - \Psi_3(t)) + A_{23}N_2\sin(\Psi_2(t) - \Psi_3(t))\right). \quad [6]$$

Each of the eight invariant manifolds is defined to be stable if solutions corresponding to initial conditions near the manifold approach the manifold with time; in this case the full dynamical solution is well approximated by the stable solution of the slow dynamics of Eq. **6**. We can determine conditions under which each of the eight manifolds is stable by computing the stability of the boundary layer dynamics (fast dynamics) evaluated at the stable solution(s) of the slow dynamics (23) (*SI Text*). Without loss of generality we set $\bar{\theta}_1 = 0$ and $0 \le \bar{\theta}_2 \le \pi$; thus, the difference in preferred directions $\bar{\theta}_2 - \bar{\theta}_1 = \bar{\theta}_2$. We focus on the case in which the two informed subgroups have equal population size; i.e., we take $N_1 = N_2$.

Our analysis shows that manifolds $\mathcal{M}_{101}$ and $\mathcal{M}_{110}$ (where the uninformed subgroup couples with only one of the coupled informed subgroups) are always unstable, but there are conditions such that the remaining six manifolds are stable. The manifolds $\mathcal{M}_{010}$ and $\mathcal{M}_{001}$ (where the uninformed subgroup couples with only one of the *uncoupled* informed subgroups) are both stable if and only if

$$\cos\bar{\theta}_2 < 2r^2 - 1,$$

i.e., if and only if the difference in preferred direction $\bar{\theta}_2 > \bar{\theta}_c$, where the critical difference in preference direction $\bar{\theta}_c$ is given by

$$\bar{\theta}_c = \cos^{-1}(2r^2 - 1). \quad [7]$$

On the other hand, manifold $\mathcal{M}_{111}$ (where all subgroups are coupled) is stable if $\bar{\theta}_2 < \bar{\theta}_c$, i.e., if

$$\cos\bar{\theta}_2 > 2r^2 - 1.$$

The dependency of the stability of the manifolds on the critical angle $\bar{\theta}_c$ can be interpreted as follows. Given a value of sensing range parameter r, for sufficiently large difference $\bar{\theta}_2$ between the two preferred directions, the two informed subgroups will be pulled enough in their preferred directions such that they will lose direct connection with each other. Depending on initial conditions the uninformed subgroup may become connected with one or the other of the two informed subgroups corresponding to the interconnections on $\mathcal{M}_{010}$ or $\mathcal{M}_{001}$ in Fig. 1. On the other hand, for sufficiently small difference $\bar{\theta}_2$ between the two preferred directions, the two informed subgroups can stay connected with each other and with the uninformed subgroup corresponding to the fully connected case of $\mathcal{M}_{111}$.

The stable solution of the slow dynamics of Eq. **6** on the manifold $\mathcal{M}_{010}$ corresponds to all of the informed individuals in subgroup 1 and all of the uninformed individuals (subgroup 3) moving steadily in the preferred direction $\bar{\theta}_1$; the informed individuals in subgroup 2 are disconnected from the greater aggregation and move off by themselves in their preferred direction $\bar{\theta}_2$. We classify this solution as (most of) the group making a decision for preference 1. Likewise, the stable solution on the manifold $\mathcal{M}_{001}$ corresponds to all of the informed individuals in subgroup 2 and all of the uninformed individuals (subgroup 3) moving steadily in the preferred direction $\bar{\theta}_2$; the informed individuals in subgroup 1 are disconnected from the greater aggregation and move off by themselves in their preferred direction $\bar{\theta}_1$. We classify this solution as (most of) the group making a decision for preference 2.

Fig. 2 shows a simulation of $N = 30$ individuals obeying the dynamics of Eqs. **1**–**4** with $N_1 = N_2 = 5$ and $N_3 = 20$. Here $r = 0.9$, which corresponds to $\bar{\theta}_c = 52^\circ$. Further, $\bar{\theta}_2 = 90^\circ$, which is greater than $\bar{\theta}_c$ so that $\mathcal{M}_{010}$ and $\mathcal{M}_{001}$ are both stable. Indeed, for the initial conditions illustrated in the plot in Fig. 2 (see also Fig. S1), the solution converges to a group decision for preference 1 as in the slow dynamics on $\mathcal{M}_{010}$.

Depending on parameters, the slow dynamics of Eq. **6** on the manifold $\mathcal{M}_{111}$, corresponding to the fully connected case, can have up to two stable solutions. In the first stable solution each of the two informed subgroups compromises between its preferred directions and the average of the two preferred directions, whereas the uninformed subgroup travels in the average of the two preferred directions. Fig. 3 shows a simulation of $N = 30$ individuals obeying the dynamics of Eqs. **1**–**4** with $N_1 = N_2 = 5$ and $N_3 = 20$. Here $r = 0.6$, which corresponds to $\bar{\theta}_c = 106^\circ$. As in the previous example, $\bar{\theta}_2 = 90^\circ$, but now this is less than $\bar{\theta}_c$ so that $\mathcal{M}_{010}$ and $\mathcal{M}_{001}$ are unstable and $\mathcal{M}_{111}$ is stable. Indeed, for the initial conditions of Fig. 3 (the same as in Fig. 2), the solution converges to the compromises as in the first stable solution of the slow dynamics on $\mathcal{M}_{111}$. If $N_3 > 2N_1$, i.e., for a sufficiently large population of uninformed individuals, $\mathcal{M}_{111}$ is attractive *only* near the first stable solution if $\bar{\theta}_2 < \bar{\theta}_c$.

The second stable solution of Eq. **6** on the manifold $\mathcal{M}_{111}$ is symmetric to the first stable solution: The uninformed subgroup moves in the direction 180° from the average of the two preferred directions and each informed subgroup compromises between this direction and its preferred direction. This is a somewhat pathological solution that is very far from a group decision. However, this second solution does not exist in the presence of a sufficiently large population of uninformed individuals, notably in the case that

$$\left(\frac{N_3}{2N_1}\right)^{2/3} > 1 - \left(\frac{2N_1K_1}{N\sin(\bar{\theta}_2/2)}\right)^{2/3}. \qquad [8]$$

Inequality Eq. **8**, which derives from our stability analysis, is always satisfied for $N_3 > 2N_1$ or for sufficiently large strength of social interactions given by $K_1 \geq 2$. Thus, under the condition $N_3 > 2N_1$, $\mathcal{M}_{111}$ is unstable precisely when $\mathcal{M}_{010}$ and $\mathcal{M}_{001}$ are stable. Fig. 4 illustrates stability of decisions (on $\mathcal{M}_{010}$ and $\mathcal{M}_{001}$) versus compromise (on $\mathcal{M}_{111}$) as a function of preference difference $\bar{\theta}_2$.

Fig. 5, *Upper Left* plots r as a function of $\bar{\theta}_2$ given by Eq. **7**; this curve defines the condition for stability of a collective decision for preference 1 as defined by the solution on $\mathcal{M}_{010}$ and for preference 2 as defined by the solution on $\mathcal{M}_{001}$. The gray region illustrates the parameter space corresponding to stability of a collective decision. The decision is unstable in the parameter space defined by the white region. Given a fixed value of r, the curve provides a lower bound on the preference difference $\bar{\theta}_2$ for which a decision is stable.

Now suppose that a number of uninformed individuals are added to the aggregation; i.e., the density is increased. For any individual to retain roughly the same number of neighbors after the addition of individuals as before, it can decrease its sensing range. A decrease in sensing range corresponds to an increase in r. As seen in Fig. 5, an increase in r corresponds to a decrease in the lower bound $\bar{\theta}_c$; i.e., with increased numbers of uninformed individuals, a collective decision is stable for lower values of preference difference $\bar{\theta}_2$.

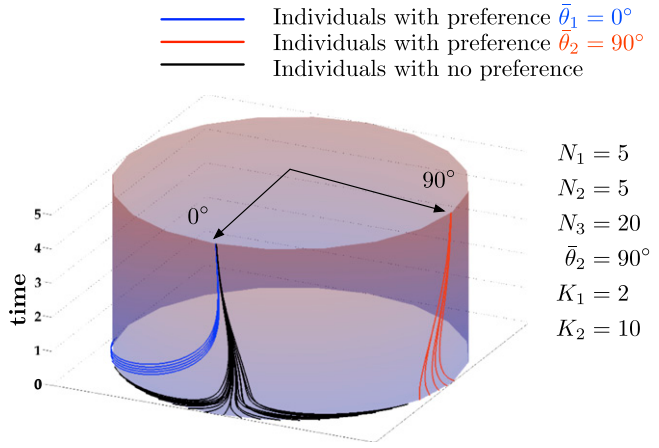

Fig. 2. Simulation of dynamics of Eqs. **1**–**4** with $N = 30$ individuals, $r = 0.9$, and $\bar{\theta}_1 = 0^\circ$ and $\bar{\theta}_2 = 90^\circ$ as shown with black arrows on the top of the cylinder. The solution for each individual is shown evolving on the surface of the cylinder; the azimuth describes the angle θ_j and the vertical axis describes time t. For this example, $\bar{\theta}_2 > \bar{\theta}_c = 52^\circ$ and it can be observed that a decision is made for preference 1.

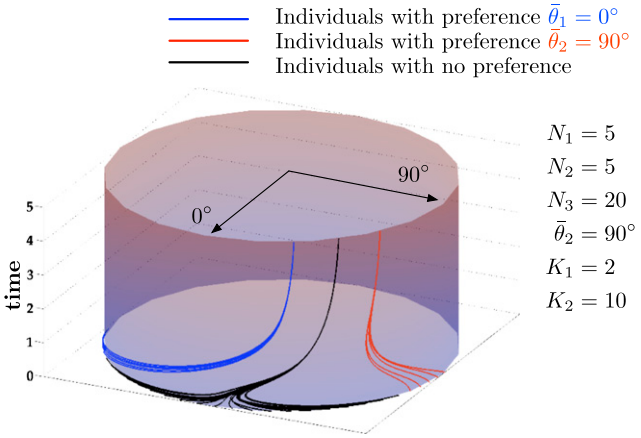

Fig. 3. Simulation of dynamics of Eqs. **1**–**4** with $N = 30$ individuals, $r = 0.6$, and $\bar{\theta}_1 = 0^\circ$ and $\bar{\theta}_2 = 90^\circ$. For this example, $\bar{\theta}_2 < \bar{\theta}_c = 106^\circ$ and it can be observed that no decision is made. Instead, the agents collect in subgroups that compromise.

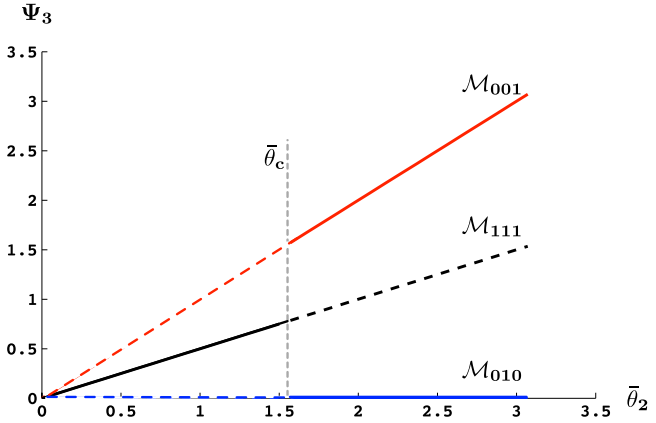

Fig. 4. Stability of decisions (on $\mathcal{M}_{010}$ and $\mathcal{M}_{001}$) versus compromise (on $\mathcal{M}_{111}$) illustrated in a plot of direction of uninformed subgroup Ψ_3 as a function of preference difference $\bar{\theta}_2$. Here $r = 0.707$ and so $\bar{\theta}_c = \pi/2$. A solid line denotes a stable solution and a dashed line denotes an unstable solution.

For some range of parameter values for which $\mathcal{M}_{010}$ and $\mathcal{M}_{001}$ are stable, it is possible that $\mathcal{M}_{000}$, $\mathcal{M}_{100}$, and/or $\mathcal{M}_{011}$ are also stable. This means that even if $\mathcal{M}_{010}$ and $\mathcal{M}_{001}$ are stable, for some initial conditions the solution may converge to the stable solutions of $\mathcal{M}_{000}$, $\mathcal{M}_{100}$, and/or $\mathcal{M}_{011}$, none of which corresponds to a collective decision for preference 1 or 2. In fact, the only stable solution on $\mathcal{M}_{000}$ corresponds to the three subgroups moving apart. $\mathcal{M}_{100}$ can have up to two stable solutions and $\mathcal{M}_{011}$ can have one stable solution; all of these correspond to compromise solutions. Therefore, we examine the conditions for stability of $\mathcal{M}_{000}$, $\mathcal{M}_{100}$, and $\mathcal{M}_{011}$ to isolate the parameter space in which $\mathcal{M}_{010}$ and $\mathcal{M}_{001}$ are the *only* stable manifolds among the eight under investigation.

The condition $\bar{\theta}_2 > \bar{\theta}_c$ is necessary for stability of $\mathcal{M}_{000}$. However, $\mathcal{M}_{000}$ is unstable as long as the initial average heading of the uninformed individuals is greater than $-\bar{\theta}_2$ and less than $2\bar{\theta}_2$, i.e., as long as the uninformed individuals are not headed in a direction that is dramatically different from the average of the two preferred directions. The latter is not so likely for initially aggregated individuals. Further, the likelihood of $\mathcal{M}_{000}$ being stable shrinks as $\bar{\theta}_2$ grows.

$\mathcal{M}_{100}$ (coupled informed subgroups) is also unstable if the initial average heading of the uninformed is not dramatically different from the average of the two preferred directions. Otherwise, if $\bar{\theta}_2 < \bar{\theta}_c$, $\mathcal{M}_{100}$ is stable about its first stable solution. The second stable solution of $\mathcal{M}_{100}$ does not exist if $K_1 < 2N/N_1$ and is not attracting if

$$r > \sqrt{1-d^2},\ d = \frac{N\sin(\bar{\theta}_2/2)}{2N_1K_1}. \qquad [9]$$

The condition $\bar{\theta}_2 > \bar{\theta}_c$ is a necessary condition for stability of $\mathcal{M}_{011}$ (uninformed coupled to uncoupled informed subgroups). However, $\mathcal{M}_{011}$ is unstable if either of the following is satisfied:

$$r < \frac{1}{\sqrt{1+\nu^2}} \text{ or } r > \sqrt{\frac{1}{2}+\frac{1}{2\sqrt{1+\nu^2}}}, \qquad [10]$$

where

$$\nu = \frac{N\sin(\bar{\theta}_2/2)}{N_3K_1 + N\cos(\bar{\theta}_2/2)}.$$

Table 1 summarizes the possible coexistence of stable manifolds for different parameter ranges, assuming $N_3 > 2N_1$. For the initial conditions we consider, $\mathcal{M}_{000}$ and $\mathcal{M}_{100}$ will be unstable, in which case, when $\mathcal{M}_{111}$ is stable, it is exclusively stable among the eight manifolds. Further, the parameter values that yield the exclusive stability of $\mathcal{M}_{010}$ and $\mathcal{M}_{001}$ among the eight invariant manifolds are those that satisfy Eq. **10**; these values are shown as dark gray regions in the parameter space plots in Fig. 5. In three plots, the green curve plots r as a function of $\bar{\theta}_2$ in the case of equality in the first condition of Eq. **10**, and the orange curve plots r as a function of $\bar{\theta}_2$ in the case of equality in the second condition of Eq. **10**. In each of the plots, $N_1 = N_2 = 5$ and $K_1 = 2$. The number of uninformed individuals N_3 ranges from $N_3 = 11$ (Fig. 5, *Upper Right*) to $N_3 = 50$ (Fig. 5, *Lower Left*) to $N_3 = 500$ (Fig. 5, *Lower Right*). The plots show the dark gray region expanding with increasing N_3; i.e., the region of parameter space that ensures unique stability of the collective decision for one or the other preference expands with increasing number of uninformed individuals. An increase in strength of social interaction K_1 also increases this parameter space.

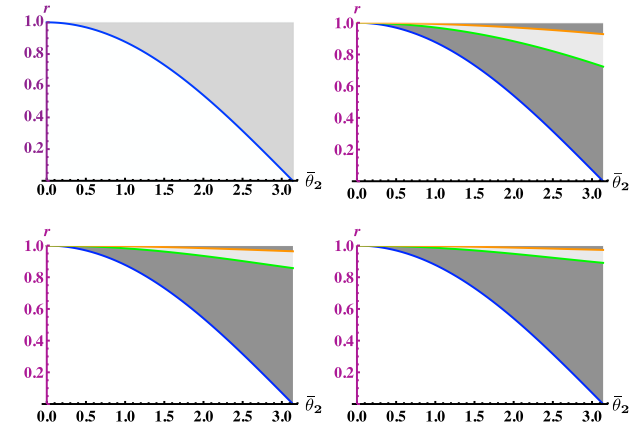

Fig. 5. Curves in the space of parameters $\bar{\theta}_2$ and r that determine the stability of manifolds $\mathcal{M}_{010}$ and $\mathcal{M}_{001}$ and, thus, the stability of a collective decision. In all plots, $K_1 = 2$ and $N_1 = N_2 = 5$. (*Upper Left*) Light gray parameter space corresponds to stability of $\mathcal{M}_{010}$ and $\mathcal{M}_{001}$, independent of N_3. (*Upper Right*) $N_3 = 11$. (*Lower Left*) $N_3 = 50$. (*Lower Right*) $N_3 = 500$. Dark gray parameter space corresponds to $\mathcal{M}_{010}$ and $\mathcal{M}_{001}$ being the only stable manifolds among the eight invariant manifolds studied. The dark gray parameter space increases with increasing number of uninformed individuals N_3.

Discussion

The continuous-time, deterministic, dynamical system model presented and analyzed in this paper approximates the decision making of a group of informed and uninformed individuals on the move as studied in ref. 1. In the case that the two informed subgroups 1 and 2 are equally sized ($N_1 = N_2$), it is shown in ref. 1 that the whole group will decide with high probability to move in one of the two preferred directions, as long as the difference in directions $\bar{\theta}_2$ is greater than some critical threshold. Otherwise, the group will compromise.

Our stripped-down model retains dynamically changing, local social interactions, but neglects some of the details of the zonal-based interaction rules of ref. 1. Nonetheless, it provides the

Table 1. Possible combinations of stable (*S*) and unstable (*U*) manifolds given $N_3 > 2N_1$

$\mathcal{M}_{101}$	$\mathcal{M}_{110}$	$\mathcal{M}_{000}$	$\mathcal{M}_{010}$	$\mathcal{M}_{001}$	$\mathcal{M}_{100}$	$\mathcal{M}_{011}$	$\mathcal{M}_{111}$
U	*U*	*S*	*S*	*S*	*U*	*U*	*U*
U	*U*	*S*	*S*	*S*	*U*	*S*	*U*
U	*U*	*S*	*S*	*S*	*S*	*U*	*U*
U	*U*	*S*	*S*	*S*	*S*	*S*	*U*
U	*U*	*U*	*U*	*U*	*S*	*U*	*S*

ECOLOGY

same fundamental result in the case $N_1 = N_2$ without requiring any additional modeling terms such as a forgetting factor on information that is not reinforced (12). Further, simulations of the continuous-time model with random terms suggest that the analysis of the deterministic model is robust to a small level of uncertainty (*SI Text* and Fig. S2). In the case $N_1 \neq N_2$, our model yields the same necessary and sufficient conditions for stability of a decision (see *SI Text* and Fig. S3 for simulations). In the case of a decision, simulations show a dominating region of attraction for the decision to move in the preferred direction of the majority informed subgroup (*SI Text* and Fig. S3), consistent with ref. 1.

A decision in the continuous-time model corresponds to one informed subgroup and the uninformed individuals choosing to move together in the same preferred direction. This decision differs slightly from the decision in ref. 1 where all individuals move together in the preferred direction. However, the result is qualitatively the same, and the continuous-time model has the advantage of analytical tractability. Indeed, the critical threshold $\bar{\theta}_c$ is explicitly defined in Eq. **7** (and illustrated in Fig. 5, *Upper Left*). This threshold provides a sharp condition for stability of the two symmetric collective decision solutions versus stability of a compromise solution. Further, the decision in ref. 1 can be recovered with the continuous-time model by the addition of a mechanism inspired by the repulsive term in the dynamics of ref. 1.

The analytical tractability of the continuous-time model allows formal investigation into the sensitivity of the decision-making results to model parameters. In particular, our analysis permits a formal examination of the role of the uninformed population size in the group decision-making dynamics. Our results provide formal evidence that an increase in uninformed population size N_3 can improve decision making for a group in motion by increasing the likelihood that the group will make a decision rather than compromise. A first supporting result concerns the second stable compromise solution on $\mathcal{M}_{111}$. This solution is worse for decision making than the first stable compromise solution because not only does the group not make a decision, but also it moves in the direction opposite the average of the two preferred directions. The presence of a sufficient number of uninformed individuals prevents such a solution, throwing off the delicate balance that is required for its existence. Further, a large enough N_3 limits the attractiveness of the first stable compromise solution, making the sufficient condition for stability of $\mathcal{M}_{111}$ also a necessary condition.

A second supporting piece of evidence derives from the result that the minimum difference in preference direction required for a group decision decreases with a decreasing sensing range (equivalently, an increasing threshold r on synchrony of directions sensed) (Eq. **7**). This result suggests that the more local the sensing is, the better the sensitivity to the conflict in preference; when individuals sense too much of the group, the result is a filtering of the local influences and an averaged (compromised) collective response. By increasing the density of the group, even by adding *uninformed* individuals, an individual can reduce its sensing range and keep track of the same number of neighbors; in such a way an increase in population size of uninformed individuals lowers the critical difference in preference direction, making a group decision more likely.

The third supporting result, illustrated in three plots in Fig. 5, shows that an increasing uninformed population size N_3 increases the region of parameter space for which a decision solution is exclusively stable among the eight solutions studied. A sufficiently large number of uninformed individuals throws off the delicate balance for the uninformed individuals to be connected to both informed subgroups without the two informed subgroups connecting with each other ($\mathcal{M}_{011}$). The uninformed individuals provide a kind of "glue"; indeed, the larger N_3 provides the same effect as increasing the social interaction strength K_1. Overall, the result shows that with larger numbers of uninformed individuals, a collective decision is more likely and more robust to variations in parameters r (sensing range) and $\bar{\theta}_2$ (difference in preferred directions).

The improvements we have shown in decision making with increased uninformed population size are striking and provide a testable result. Adding individuals that do not invest directly in an external preference provides a low-cost way in which groups can enhance decision making. Our analysis addresses the symmetric case of a group in motion in which there are two equally sized informed subgroups, each preferring to move in one of two alternative directions. Our results on stability of decision versus compromise persist in the case of unequal sized informed subgroups. In related work (24), we study the influence of uninformed individuals in the case that there is heterogeneity among informed individuals in the strength of their response to preference relative to social interactions.

ACKNOWLEDGMENTS. This research was supported in part by Office of Naval Research Grant N00014-09-1-1074 (to N.E.L., T.S., L.S., and I.D.C.), Air Force Office of Scientific Research Grant FA9550-07-1-0-0528 (to N.E.L., B.N., and L.S.), Defense Advanced Research Planning Agency Grant HR0011-09-1-0055 (to S.A.L., N.E.L., and I.D.C.), and Army Research Office Grant W911NG-11-1-0385 (to N.E.L., I.D.C., and S.A.L.).

1. Couzin ID, Krause J, Franks NR, Levin SA (2005) Effective leadership and decision-making in animal groups on the move. *Nature* 433:513–516.
2. Krause J, Ruxton GD (2002) *Living in Groups* (Oxford Univ Press, Oxford).
3. Couzin ID, Krause J (2003) Self-organization and collective behaviour in vertebrates. *Adv Stud Behav* 32:1–75.
4. Franks NR, Pratt SC, Mallon EB, Britton NF, Sumpter DJT (2002) Information flow, opinion polling and collective intelligence in house-hunting social insects. *Philos Trans R Soc Lond B Biol Sci* 357:1567–1583.
5. Lindauer M (1957) Communication in swarm-bees searching for a new home. *Nature* 179:63–67.
6. Seeley TD (2003) Consensus building during nest-site selection in honey bee swarms: The expiration of dissent. *Behav Ecol Sociobiol* 53:417–424.
7. Reebs SG (2000) Can a minority of informed leaders determine the foraging movements of a fish shoal? *Anim Behav* 59:403–409.
8. Biro D, Sumpter DJT, Meade J, Guilford T (2006) From compromise to leadership in pigeon homing. *Curr Biol* 16:2123–2128.
9. Mauboussin MJ (2006) *More Than You Know: Finding Wisdom in Unconventional Places* (Columbia Univ Press, New York).
10. Krause J, Ruxton GD, Krause S (2010) Swarm intelligence in animals and humans. *Trends Ecol Evol* 25:28–34.
11. Couzin ID (2009) Collective cognition in animal groups. *Trends Cogn Sci* 13:36–43.
12. Nabet B, Leonard NE, Couzin ID, Levin SA (2009) Dynamics of decision making in animal group motion. *J Nonlinear Sci* 19:399–435.
13. Nabet B (2009) Dynamics and control in natural and engineered multi-agent systems. PhD thesis (Princeton Univ, Princeton).
14. Vicsek T, Czirók A, Ben-Jacob E, Cohen I, Shochet O (1995) Novel type of phase transition in a system of self-driven particles. *Phys Rev Lett* 75:1226–1229.
15. Kuramoto Y (1984) *Chemical Oscillations, Waves, and Turbulence* (Springer, Berlin).
16. Strogatz SH (2000) From Kuramoto to Crawford: Exploring the onset of synchronization in populations of coupled oscillators. *Physica D* 143:1–20.
17. Sepulchre R, Paley D, Leonard NE (2008) Stabilization of planar collective motion with limited communication. *IEEE Trans Automat Contr* 53:706–719.
18. Justh E, Krishnaprasad PS (2004) Equilibria and steering laws for planar formations. *Syst Control Lett* 52:25–38.
19. Mirollo RE, Strogatz SH (1990) Jump bifurcation and hysteresis in an infinite-dimensional dynamical system of coupled spins. *SIAM J Appl Math* 50:108–124.
20. Cucker F, Smale S (2007) Emergent behavior in flocks. *IEEE Trans Automat Contr* 52: 852–862.
21. Abbott LF, Nelson SB (2000) Synaptic plasticity: Taming the beast. *Nat Neurosci* 3 (Suppl):1178–1183.
22. Moon SJ, Nabet B, Leonard NE, Levin SA, Kevrekidis IG (2007) Heterogeneous animal group models and their group-level alignment dynamics: An equation-free approach. *J Theor Biol* 246:100–112.
23. Kokotovic PV, Khalil HK, O'Reilly J (1986) *Singular Perturbations Methods in Control: Analysis and Design* (Academic, New York).
24. Couzin ID, et al. (2011) Uninformed individuals promote democratic consensus in animal groups. *Science*, in press.

Supporting Information

Leonard et al. 10.1073/pnas.1118318108

SI Text

Model Reduction. To formalize the timescale separation, we define a coordinate transformation from the original $N+\frac{N(N-1)}{2}$ variables to a new set of independent variables that distinguishes between slow and fast variables. The original variables (defined in the main text) include the direction of motion of each of the N individuals $\theta_j, j = 1, \ldots, N$, and the $\frac{N(N-1)}{2}$ independent social interaction weights $a_{jl}, j = 1, \ldots, N, l = j + 1, \ldots, N$.

Let $\mathcal{N}_k' \subset \mathcal{N}_k$ denote the set of $N_k - 1$ indexes in $\mathcal{N}_k$ corresponding to the individuals in subgroup k excluding the individual with the largest index. Let $i = \sqrt{-1}$. For each $j \in \mathcal{N}_k'$ and each $k = 1, 2, 3$, we define the complex variable α_j as follows:

$$\alpha_j = \cos\left(N_k\theta_j - \sum_{l\in\mathcal{N}_k}\theta_l\right) + i\sin\left(N_k\theta_j - \sum_{l\in\mathcal{N}_k}\theta_l\right). \quad [S1]$$

The variable α_j quantifies how close the direction of motion of individual j is to the average direction of motion of its subgroup Ψ_k. When all individuals in subgroup k move in the same direction, $\alpha_j = 1$ for every $j \in \mathcal{N}_k'$. We define the new set of independent variables by the $N + \frac{N(N-1)}{2}$ set of variables (Ψ_k, α_j, a_{jl}). That this change of variables is well defined near the invariant manifolds described below is proved in ref. 1.

Let $\varepsilon = \max\left(\frac{1}{K_1}, \frac{1}{K_2}\right)$. Eqs. **1**–**4** from the main text can be written with respect to the new variables as

$$\frac{d\Psi_1}{dt} = \frac{1}{N_1\rho_1}\sum_{l\in\mathcal{N}_1}\left(\sin(\bar\theta_1 - \theta_l) + \frac{K_1}{N}\left(\sum_{n=1}^{N} a_{ln}\sin(\theta_n - \theta_l)\right)\right)\cos(\Psi_1 - \theta_l), \quad [S2]$$

$$\frac{d\Psi_2}{dt} = \frac{1}{N_2\rho_2}\sum_{l\in\mathcal{N}_2}\left(\sin(\bar\theta_2 - \theta_l) + \frac{K_1}{N}\left(\sum_{n=1}^{N} a_{ln}\sin(\theta_n - \theta_l)\right)\right)\cos(\Psi_2 - \theta_l), \quad [S3]$$

$$\frac{d\Psi_3}{dt} = \frac{1}{N_3\rho_3}\sum_{l\in\mathcal{N}_3}\left(\frac{K_1}{N}\left(\sum_{n=1}^{N} a_{ln}\sin(\theta_n - \theta_l)\right)\right)\cos(\Psi_3 - \theta_l), \quad [S4]$$

$$\varepsilon\frac{d\alpha_j}{dt} = iN_1\alpha_j\left(\varepsilon\left(\sin(\bar\theta_1 - \theta_j) - \rho_1\sin(\bar\theta_1 - \Psi_1)\right) + \frac{\varepsilon K_1}{N}\left(\sum_{n=1}^{N} a_{jn}\sin(\theta_n - \theta_j) - \frac{1}{N_1}\sum_{l\in\mathcal{N}_1}\sum_{n=1}^{N} a_{ln}\sin(\theta_n - \theta_l)\right)\right), j \in \mathcal{N}_1' \quad [S5]$$

$$\varepsilon\frac{d\alpha_j}{dt} = iN_2\alpha_j\left(\varepsilon\left(\sin(\bar\theta_2 - \theta_j) - \rho_2\sin(\bar\theta_2 - \Psi_j)\right) + \frac{\varepsilon K_1}{N}\left(\sum_{n=1}^{N} a_{jn}\sin(\theta_n - \theta_j) - \frac{1}{N_2}\sum_{l\in\mathcal{N}_2}\sum_{n=1}^{N} a_{ln}\sin(\theta_n - \theta_l)\right)\right), j \in \mathcal{N}_2' \quad [S6]$$

$$\varepsilon\frac{da_j}{dt} = iN_3\alpha_j\left(\frac{\varepsilon K_1}{N}\left(\sum_{n=1}^{N} a_{jn}\sin(\theta_n - \theta_j) - \frac{1}{N_3}\sum_{l\in\mathcal{N}_3}\sum_{n=1}^{N} a_{ln}\sin(\theta_n - \theta_l)\right)\right), j \in \mathcal{N}_3' \quad [S7]$$

$$\varepsilon\frac{da_{lj}}{dt} = \varepsilon K_2(1 - a_{lj})a_{lj}\left(\rho_{lj} - r\right), l \in \{1, \ldots, N\}, j \in \{l+1, \ldots, N\}, \quad [S8]$$

for $\rho_k \neq 0$, $k = 1, 2, 3$.

For $\varepsilon \ll 1$, we have that εK_1 and εK_2 are of order of magnitude 1. We also assume that N_k/N and $K_1/(NN_k)$ are of order of magnitude 1. Then, the model of Eqs. **S2**–**S8** has the form of a standard singular perturbation model (2):

$$\frac{d\mathbf{x}}{dt} = \mathbf{f}(\mathbf{x}, \mathbf{z}, \varepsilon) \quad [S9]$$

$$\varepsilon\frac{d\mathbf{z}}{dt} = \mathbf{g}(\mathbf{x}, \mathbf{z}, \varepsilon), \quad [S10]$$

where $\mathbf{x}$ is the vector of the three slow variables Ψ_k and $\mathbf{z}$ is the $N - 3 + \frac{N(N-1)}{2}$ vector of fast variables (α_j, a_{jl}). Each of the eight invariant manifolds $\mathcal{M}_{101}$, $\mathcal{M}_{110}$, $\mathcal{M}_{000}$, $\mathcal{M}_{010}$, $\mathcal{M}_{001}$, $\mathcal{M}_{100}$, $\mathcal{M}_{011}$, and $\mathcal{M}_{111}$, described in the main text, is computed as an isolated equilibrium solution of the fast dynamics given by Eqs. **S5**–**S8** when $\varepsilon = 0$, i.e., an isolated solution $\mathbf{z} = \mathbf{h}(\mathbf{x})$ of $\mathbf{g} = (\mathbf{x}, \mathbf{z}, 0) = 0$. These eight solutions correspond to $\alpha_j = 1$ for all j, which implies that $\rho_k = 1$ and $\theta_j = \Psi_k$ for $j \in \mathcal{N}_k$ and $k = 1, 2, 3$. Additionally, $a_{jl} \in \{0, 1\}$ for all j, l, and in particular $a_{jl} = 1$ when $j \in \mathcal{N}_k$ and $l \in \mathcal{N}_k$. If $j \in \mathcal{N}_m$ and $l \in \mathcal{N}_n$, $m \neq n$, then $a_{jl} = A_{nm}$.

The reduced dynamics on each invariant manifold (Eq. **6** in the main text) are derived by substituting the corresponding isolated solution into the slow dynamics given by Eqs. **S2**–**S4**; i.e., $d\mathbf{x}/dt = \mathbf{f}(\mathbf{x}, \mathbf{h}(\mathbf{x}), 0)$. These dynamics are gradient dynamics; i.e., they can be written in the form

$$\frac{d\Psi_k}{dt} = -\frac{\partial V}{\partial\Psi_k}, k = 1, 2, 3,$$

where $V = V(\Psi_1, \Psi_2, \Psi_3)$. As a result, all equilibrium solutions on each manifold are critical points of V and there are no periodic solutions. An equilibrium solution on a manifold is (exponentially) stable if the eigenvalues of the Jacobian of the reduced dynamics evaluated at that equilibrium all have strictly negative real part.

Stability of Invariant Manifolds. To determine the (local) stability of each of the eight invariant manifolds, we check stability of the boundary layer equations about each stable solution on the manifold. The boundary layer equations can be computed from the fast dynamics Eqs. **S5**–**S8** as described in ref. 2. An invariant manifold is stable, i.e., locally attractive near a stable solution on the manifold, if the boundary layer dynamics are locally exponentially stable near the stable solution on the manifold, uniformly in the slow variables (Ψ_1, Ψ_2, Ψ_3). Here, conditions for local exponential stability can be proved by showing that the eigenvalues of the Jacobian of the boundary layer equations evaluated at the stable solution on the manifold have strictly

negative real part. Singular perturbation theory then guarantees that solutions to the full dynamics starting close to the stable solution on the invariant manifold stay close to solutions of the reduced dynamics. See ref. 2 for details.

Stability of any of the invariant manifolds is satisfied if and only if the following six terms are all negative when evaluated at the equilibrium solution on the manifold,

$$-\frac{1}{N}\left(1-\frac{1}{N_k}\right)\left(N_k+\sum_{l\neq k}N_m A_{km}\cos(\Psi_m-\Psi_k)\right),\ k=1,2,3, \quad \textbf{[S11]}$$

and $(1-2A_{12})(\rho_{12}-r)$, $(1-2A_{13})(\rho_{13}-r)$, $(1-2A_{23})(\rho_{23}-r)$, where $\rho_{km}=|\cos(\frac{1}{2}(\Psi_k-\Psi_m))|$.

As an example, consider the manifold $\mathcal{M}_{010}$, where $A_{13}=1$ and $A_{12}=A_{23}=0$. The only stable solution on this manifold is $(\Psi_1, \Psi_2, \Psi_3)=(0,\bar{\theta}_2,0)$, because $\bar{\theta}_1=0$. Evaluating the sign of the six terms above at this equilibrium implies that $\mathcal{M}_{010}$ is stable if and only if

$$\left|\cos\left(\frac{\bar{\theta}_2}{2}\right)\right|-r<0,$$

which is equivalent to $\cos\bar{\theta}_2<2r^2-1$, the condition cited in the main text.

Initial Conditions. Fig. S1 shows the initial direction of motion $\theta_j(0)$ for individuals $j=1,\ldots,N$, used in the simulations in Figs. 2 and 3 in the main text and the simulations in Figs. S2 and S3. All initial values of interaction gains $a_{lj}(0)$ are taken from a uniform distribution with mean = 0.2 and SD = 0.1.

Randomness. Fig. S2 shows two simulations of the dynamics of Eqs. **1–4** in the main text with the same initial conditions and parameter values as for the simulations shown in Figs. 2 and 3 in the main text, but with randomness added. For each j, we let w_j be an independent random variable drawn from a uniform distribution with mean = 0 and SD = 0.5. Eqs. **1–3** from the main text are modified to include a random term as follows:

$$\frac{d\theta_j}{dt}=\sin(\bar{\theta}_1-\theta_j)+\frac{K_1}{N}\sum_{l=1}^{N}a_{jl}\sin(\theta_l-\theta_j)+w_j,\ j \text{ in subgroup 1}$$
$$\frac{d\theta_j}{dt}=\sin(\bar{\theta}_2-\theta_j)+\frac{K_1}{N}\sum_{l=1}^{N}a_{jl}\sin(\theta_l-\theta_j)+w_j,\ j \text{ in subgroup 2}$$
$$\frac{d\theta_j}{dt}=\frac{K_1}{N}\sum_{l=1}^{N}a_{jl}\sin(\theta_l-\theta_j)+w_j,\ j \text{ in subgroup 3}. \quad \textbf{[S12]}$$

Fig. S2 exhibits the same net behavior as in the case with no randomness; i.e., for $r=0.9$ a decision is made for preference 1 and for $r=0.6$ there is a compromise solution. The use of uniform noise is a conservative choice for examining robustness because compared with Gaussian noise it gives a higher probability of large random deviations.

Asymmetric Informed Populations. Fig. S3 shows simulations of the dynamics of Eqs. **1–4** from the main text with the same initial conditions and parameter values as for the simulations shown in Figs. 2 and 3, but for an asymmetry in the sizes of the informed subgroups. Here we let $N_1=4$ and $N_2=6$. In Fig. S3, *Left* as in Fig. 2, $r=0.9$ and a decision is made. In Fig. S3, *Right* as in Fig. 3, $r=0.6$ and a compromise is made. Whereas in the simulation in Fig. 2, the solution is attracted to the manifold $\mathcal{M}_{010}$ where a decision for preference 1 is made, in the simulation in Fig. S3, *Left* with $N_2>N_1$, the solution is attracted to the manifold $\mathcal{M}_{001}$ where a decision for preference 2 is made.

1. Nabet B (2009) *Dynamics and Control in Natural and Engineered Multi-Agent Systems.* PhD thesis (Princeton University, Princeton).

2. Khalil HK (1992) *Nonlinear Systems* (Macmillan, New York).

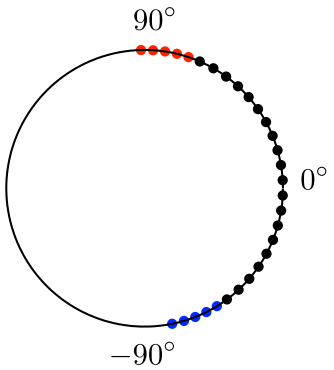

Fig. S1. The initial direction of motion $\theta_j(0)$ for each $j=1,\ldots,N$ is displayed on the unit circle. The $\theta_j(0)$ are evenly distributed between −78.5° and −58.5° for the $N_1=5$ individuals in subgroup 1 (blue circles), between 71.5° and 91.5° for the $N_2=5$ individuals in subgroup 2 (red circles), and between −53.5° and 66.5° for the $N_3=20$ individuals in subgroup 3 (black circles).

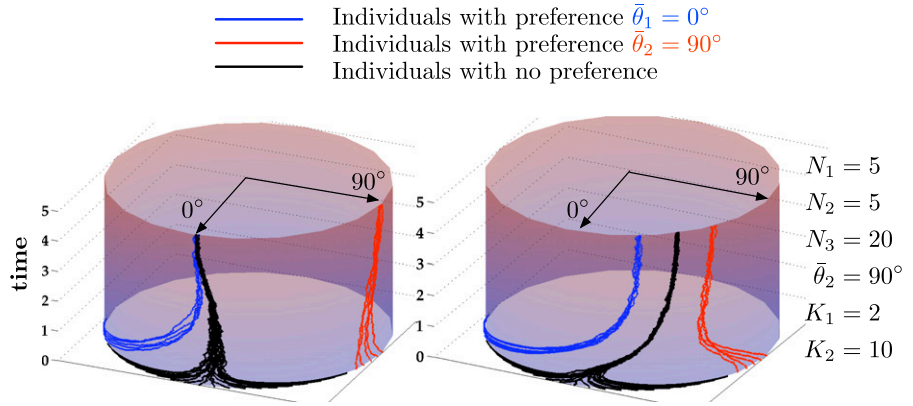

Fig. S2. Simulation of dynamics of Eqs. **1–4** from the main text modified by additive randomness as given by Eq. **S12**. (*Left*) $r = 0.9$; (*Right*) $r = 0.6$. The solution for each individual is shown evolving on the surface of the cylinder; the azimuth describes the angle θ_j and the vertical axis describes time t. Blue corresponds to subgroup 1, red to subgroup 2, and black to subgroup 3. Initial conditions and parameter values are the same as in Figs. 2 and 3 in the main text.

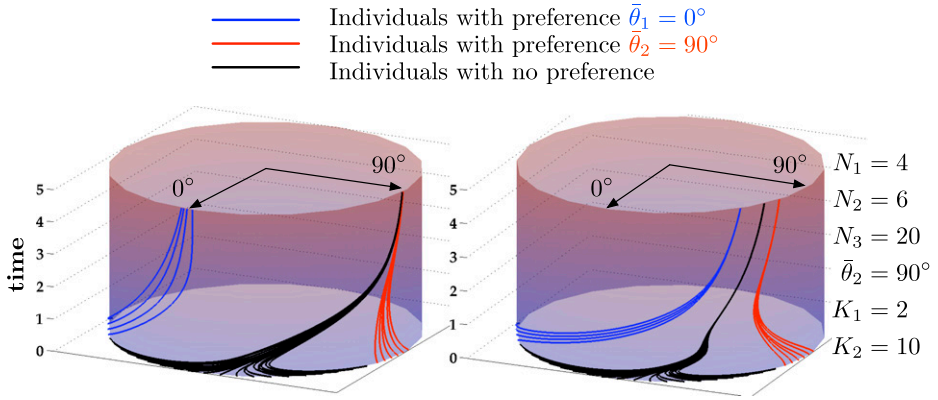

Fig. S3. Simulation of dynamics of Eqs. **1–4** from the main text with informed subgroup sizes $N_1 = 4$ and $N_2 = 6$. Initial conditions and all other parameters are the same as in Figs. 2 and 3 in the main text. (*Left*) $r = 0.9$ and the decision is made for preference 2. (*Right*) $r = 0.6$ and a compromise is made between the two preferred directions and slightly closer to preference 2.